Langmuir
Article
pubs.acs.org/Langmuir

Molecular Simulation of Nitrogen Adsorption in Nanoporous Silica

B. Coasne,*,† A. Galarneau,† F. Di Renzo,† and R. J. M. Pellenq‡,§

†*Institut Charles Gerhardt Montpellier, UMR 5253 CNRS/UM2/ENSCM/UM1, ENSCM, 8 rue de l'Ecole Normale, 34296 Montpellier Cedex 05, France,* ‡*Centre Interdisciplinaire des Nanosciences de Marseille, CNRS UPR 7251, Campus de Luminy, 13288 Marseille Cedex 09, France, and* §*Department of Civil and Environmental Engineering, Massachusetts Institute of Technology, 77 Massachusetts Avenue, Cambridge, Massachusetts 02139*

Received February 20, 2010. Revised Manuscript Received April 28, 2010

This article reports on a molecular simulation study of nitrogen adsorption and condensation at 77 K in atomistic silica cylindrical nanopores (MCM-41). Two models are considered for the nitrogen molecule and its interaction with the silica substrate. In the "pea" model, the nitrogen molecule is described as a single Lennard-Jones sphere and only Lennard-Jones interactions between the nitrogen molecule and the oxygens atoms of the silica substrate are taken into account. In the "bean" model (TraPPE force field), the nitrogen molecule is composed of two Lennard-Jones sites and a linear array of three charges on the atomic positions and at the center of the nitrogen−nitrogen bond. In the bean model, the interactions between the sites on the nitrogen molecule and the Si, O, and H atoms of the substrate are the sum of the Coulombic and dispersion interactions with a repulsive short-range contribution. The data obtained with the pea and bean models in silica nanopores conform to the typical behavior observed in the experiments for adsorption/condensation in cylindrical MCM-41 nanopores; the adsorbed amount increases continuously in the multilayer adsorption regime until an irreversible jump occurs because of capillary condensation and evaporation of the fluid within the pore. Our results suggest that the pea model can be used for characterization purposes where one is interested in capturing the global experimental behavior upon adsorption and desorption in silica nanopores. However, the bean model is more suitable to investigating the details of the interaction with the surface because this model, which accounts for the partial charges located on the nitrogen atoms of the molecule (quadrupole), allows a description of the specific interactions between this adsorbate and silica surfaces (silanol groups and siloxane bridges) or grafted silica surfaces. In particular, the bean model provides a more realistic picture of nitrogen adsorption in the vicinity of silica surfaces or confined in silica nanopores, where the isosteric heat of adsorption curves show that the nitrogen molecule in this model is sensitive to the surface heterogeneity.

1. Introduction

Fluids confined within nanometric pores (the size of a few molecular diameters) exhibit properties that are significantly different from bulk properties. In particular, nanoconfinement, surface forces, and reduced dimensions of the system affect phase transitions (condensation, freezing, etc.). Understanding such confinement and surface effects on the thermodynamics of fluids is of crucial interest for both fundamental research and potential applications. Siliceous porous materials (porous glasses and micelle-templated porous solids) are an important family of nanoporous solids because of their use as adsorbents and catalytic supports for gas adsorption, phase separation, catalysis, the preparation of nanostructured materials, and so forth.[1−3] Among porous silicas, micelle-templated materials such as MCM-41,[4] MCM-48,[4] and SBA-15[5] have attracted a great deal of attention because of their simple pore morphology (pore shape) and topology (pore connectivity) compared to those of other porous silicas (controlled pore glass and Vycor). These micelle-templated materials are obtained by a template mechanism involving the formation of surfactant or block copolymer micelles in a mixture composed of a solvent and a silica source. Polymerization of the silica and removal of the organic micelles lead to a material presenting an array of regular pores. The pore diameter distribution is narrow with an average value that can be varied from 2 up to 20 nm, depending on the synthesis conditions.[3] As a result, micelle-templated porous silicas are considered to be model materials for investigating the effect of nanoconfinement on the thermodynamics and dynamics of fluids, and a large quantity of experimental, simulation, and theoretical work has been reported on gas adsorption and capillary condensation in these solids. (For a review, see refs 6 and 7.)

The adsorption of fluids in nanoporous materials still attracts a great deal of attention because they are involved in many industrial processes (catalysis, phase separation, etc.). Nitrogen adsorption experiments at low temperature are also routinely used for the characterization of porous solids.[8] For instance, the adsorbed amounts at low pressures are used to estimate, through the BET model,[9] the specific surface area of the sample as well as the characteristic difference between the substrate/fluid and the

*To whom correspondence should be addressed. E-mail: benoit.coasne@enscm.fr. Phone: +33 4 67 16 34 59. Fax: +33 4 67 16 34 70.

(1) Corma, A. *Chem. Rev.* **1997**, *97*, 2373.
(2) Ciesla, U.; Schüth, F. *Microporous Mesoporous Mater.* **1999**, *27*, 131.
(3) Soler-Illia, G. J.; de, A. A.; Sanchez, C.; Lebeau, B.; Patarin, J. *Chem. Rev.* **2002**, *102*, 4093.
(4) Beck, J. S.; Vartulli, J. C.; Roth, W. J.; Leonowicz, M. E.; Kresge, C. T.; Schmitt, K. D.; Chu, C. T.-W.; Olson, D. H.; Sheppard, E. W.; McCullen, S. B.; Higgins, J. B.; Schlenker, J. L. *J. Am. Chem. Soc.* **1992**, *114*, 10834.
(5) Zhao, D.; Feng, J.; Huo, Q.; Melosh, N.; Fredrickson, G. H.; Chmelka, B. F.; Stucky, G. D. *Science* **1998**, *279*, 548.
(6) Gelb, L. D.; Gubbins, K. E.; Radhakrishnan, R.; Sliwinska-Bartkowiak, M. *Rep. Prog. Phys.* **1999**, *62*, 1573–1659.
(7) Alba-Simionesco, C.; Coasne, B.; Dosseh, G.; Dudziak, G.; Gubbins, K. E.; Radhakrishnan, R.; Sliwinska-Bartkowiak, M. *J. Phys.: Condens. Matter* **2006**, *18*, R15.
(8) Rouquerol, F.; Rouquerol, J.; Sing, K. S. W. *Adsorption by Powders and Porous Solids*; Academic Press: London, 1999.
(9) Brunauer, S.; Emmett, P. H.; Teller, E. *J. Am. Chem. Soc.* **1938**, *60*, 309.

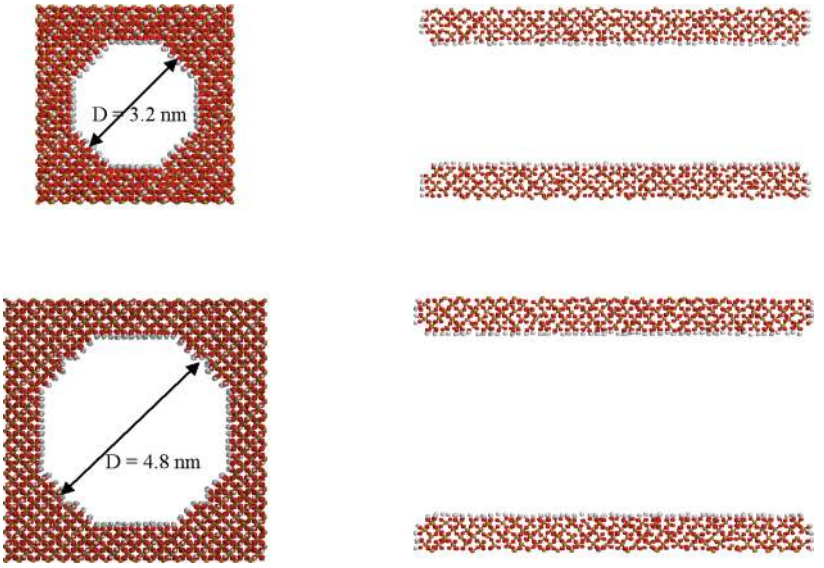

Figure 1. Plane and transverse views of atomistic silica cylindrical nanopores with different diameters: (top) $D = 3.2$ nm and (bottom) $D = 4.8$ nm. The orange and red spheres are the silicon and oxygen atoms, respectively. The white spheres are the hydrogen atoms that delimit the pore surface. Note that the pores are of a finite length so that they are open at both ends toward an external bulk reservoir. Silica nanopores with $D = 3.2$ and 4.8 nm were carved out of initial silica blocks with dimensions of 4.9 nm $\times$4.9 nm $\times$15.0 nm and 6.4 nm $\times$6.4 nm $\times$15.0 nm, respectively.

fluid/fluid interaction energies. Other methods such as the t-plot method[8] are used to estimate the surface roughness or microporosity of the sample by comparing the amount adsorbed at low pressure with some reference data obtained for macroporous solids. Nitrogen adsorption experiments are also used to estimate the pore size distribution of the sample from the capillary condensation and evaporation pressures.[8,10]

The aim of the present work is to investigate by means of molecular simulation the adsorption of nitrogen at 77 K in atomistic models of MCM-41 regular cylindrical nanopores with different pore diameters: $D = 3.2$ and 4.8 nm. Nitrogen was selected because it corresponds to a standard fluid for the adsorption-based characterization of porous solids. Two models are considered for the nitrogen molecule and its interaction with the silica substrate: the "pea" model and the "bean" model. In the pea model, the nitrogen molecule is described as a single Lennard-Jones sphere and only Lennard-Jones interactions between the nitrogen molecule and the oxygens atoms of the silica substrate are taken into account.[11] The bean model is based on the work of Potoff and Siepmann,[12] who developed a transferable potential for the phase equilibria (TraPPE) force field. In this model, the nitrogen molecule is composed of two Lennard-Jones sites and a linear array of three charges on the atom position and at the center of the nitrogen−nitrogen bond. In the bean model, the interactions between the sites on the nitrogen molecule and the Si, O, and H atoms of the silica nanopore are calculated using the PN-TraZ potential as reported for rare gas adsorption in zeolites[13] or in porous silica glass.[14] The intermolecular energy is written as the sum of the Coulombic and dispersion interactions with a repulsive short-range contribution. For both MCM-41 nanopores considered in this work, the data for the bean and pea models are analyzed and compared in terms of adsorption isotherms and isosteric heat curves. An inspection of typical molecular configurations also provides information regarding the filling and emptying mechanisms. We also discuss the structure of confined nitrogen by determining radial density profiles and pair correlation functions $g(r)$. Finally, we discuss, in light of our data, the use of characterization methods to determine the specific surface area and pore size distribution of silica samples. The remainder of the article is organized as follows. In section 2, we present the two models considered in this work for the nitrogen molecule and its interaction with the silica substrate. We also introduce the model of MCM-41 nanopores used in this work and briefly discuss the details of the simulation techniques. In section 3, we report results for the adsorption, condensation, and evaporation of nitrogen at 77 K in the silica nanoporous materials. Section 4 contains concluding remarks.

2. Computational Details

2.1. Preparation of Silica Nanopores. MCM-41 pores were described in this work as an atomistic model of cylindrical silica nanopores with different pore diameters, $D = 3.2$ and 4.8 nm (Figure 1). The latter were generated according to the following method that can be used to prepare pores of various morphologies and topologies, such as cylindrical, hexagonal, ellipsoidal, and constricted pores.[14−17] The porosity of the material can be defined using a mathematical function $\eta(x, y, z)$ that equals 1 if (x, y, z) belongs to the silica wall and 0 if (x, y, z) belongs to the void.[15,18] The nanopores used in this work were obtained by carving out of an atomistic block of cristobalite (crystalline silica) a void corresponding to $\eta(x, y, z) = 0$. All of the pores considered in this work are of a finite length $L = 10$ nm and are connected to bulk reservoirs so that they mimic real materials in which the confined fluid is always in contact with the external gas phase. (This departs from infinitely long pores for which the evaporation

(10) Barrett, E. P.; Joyner, L. G.; Halenda, P. P. *J. Am. Chem. Soc.* **1951**, *73*, 373.
(11) Brodka, A.; Zerda, T. W. *J. Chem. Phys.* **1991**, *85*, 3710.
(12) Potoff, J. J.; Siepmann, J. I. *AIChE J.* **2001**, *47*, 1676.
(13) Pellenq, R. J. M.; Nicholson, D. *J. Phys. Chem.* **1994**, *98*, 13339.
(14) Pellenq, R. J. M.; Levitz, P. E. *Mol. Phys.* **2002**, *100*, 2059.
(15) Coasne, B.; Hung, F. R.; Pellenq, R. J. M.; Siperstein, F. R.; Gubbins, K. E. *Langmuir* **2006**, *22*, 194.
(16) Coasne, B.; Galarneau, A.; Di Renzo, F.; Pellenq, R. J. M. *Langmuir* **2006**, *22*, 11097.
(17) Coasne, B.; Di Renzo, F.; Galarneau, A.; Pellenq, R. J. M. *Langmuir* **2008**, *24*, 7285.
(18) Bhattacharya, S.; Coasne, B.; Hung, F. R.; Gubbins, K. E. *Langmuir* **2009**, *25*, 5802.

Table 1. Lennard-Jones Interaction Parameters for the Pea Model of the Nitrogen Molecules and the Nitrogen Molecules' Interactions with the Oxygen Atoms of the Silica Substrate[a]

σ_{N_2/N_2}	3.75 Å
ε_{N_2/N_2}	95.2 K
$\sigma_{N_2/O}$	3.225 Å
$\varepsilon_{N_2/O}$	147.97 K

[a] From ref 11.

of the confined liquid necessarily occurs through cavitation because there is no interface with the external phase.) To mimic the silica surface in a realistic way, we removed in a second step the Si atoms that are in an incomplete tetrahedral environment. We then removed all oxygen atoms that are nonbonded. This procedure ensures that (1) the remaining silicon atoms have no dangling bonds and (2) the remaining oxygen atoms have at least one saturated bond with a Si atom. Then, the electroneutrality of the simulation box was ensured by saturating all oxygen dangling bonds with hydrogen atoms. The latter are placed in the pore void at a distance of 1 Å from the unsaturated oxygen atom along the direction perpendicular to the silica surface. It has been shown that the density of OH groups obtained using such a procedure (7−8 OH per nm^2) is close to the experimental value for porous silica glasses such as Vycor (5−7 OH per nm^2).[19−21] Then, we slightly and randomly displace all of the O, Si, and H atoms in order to mimic an amorphous silica surface. (The maximum displacement in each direction x, y, and z is 0.7 Å.)

2.2. Models for the Nitrogen Molecule and Silica−Adsorbate Interaction. Two models were considered for the nitrogen molecule and its interaction with the silica substrate: the pea and bean models.

2.2.1. Pea Model. In the first model considered in this work, nitrogen was described as a single Lennard-Jones sphere with the following parameters: σ = 3.75 Å and ε = 95.2 K.[11] No Coulombic interactions is taken into account because the atoms of the nitrogen molecule are not explicitely described in this model. The Lennard-Jones parameters for the oxygen atoms of the silica substrate are σ = 2.7 Å and ε = 230 K, and following previous simulations of nitrogen adsorption in silica gels or controlled pore glasses, we neglect interactions with silicon and hydrogen atoms of the substrate because of the low polarizability.[11,22,23] The cross-parameters for the interaction between the nitrogen molecules and the oxygen atoms of the pores were determined using the Lorentz−Berthelot mixing rules: σ = 3.225 Å and ε = 147.97 K (Table 1).

2.2.2. Bean Model. In the second model considered in this work, nitrogen was described using the model of Potoff and Siepmann.[12] In this model (Table 2), each nitrogen atom of the rigid nitrogen molecule is a center of repulsion/dispersion interactions that interact through a Lennard-Jones potential with the following parameters: σ = 3.31 Å and ε = 36 K. In addition, each nitrogen atom possesses a partial charge with q = −0.482 that interacts through Coulombic forces. At the center of the nitrogen−nitrogen bond (the N−N interatomic distance is 1.1 Å), a partial charge of q = +0.964 compensates for the negative charge on the nitrogen atoms. As pointed out by Herdes et al.,[24] such a charge distribution reproduces the measured quadrupole moment of the nitrogen molecule. Interactions between the sites on the

Table 2. Geometry and Parameters for Potential Functions for the Bean Model of the Nitrogen Molecule[a,b]

r(NN)	1.1 Å
q(N)	−0.482
σ	3.31 Å
ε	36 K

[a] From ref 12. [b] The negative charge on the nitrogen atoms is compensated for by a positive charge of q = +0.964 located at the center of the nitrogen−nitrogen bond.

nitrogen molecule and the Si, O, and H atoms of the silica nanopore were calculated using the PN-TraZ potential as reported for rare gas adsorption in a zeolite[13] or in porous silica glass.[25] The intermolecular energy is written as the sum of the Coulombic and dispersion interactions with a repulsive short-range contribution. The choice of the PN-TrAZ model to describe the benzene/silica interaction was motivated by the good transferability of this model in the case of water[26,27] and benzene in porous silica.[28,29] The adsorbate−surface energy $U_k(r_k)$ of site k of an adsorbate molecule at position r_k is given in atomic units

$$U_k(r_k) = \sum_{j=\{O,\,Si,\,H\}} \left[A_{kj} \exp(-b_{kj} r_{kj}) - \sum_{n=3}^{5} f_{2n}(r_{kj}) \frac{C_{2n}^{kj}}{r_{kj}^{2n}} + \frac{q_i q_k}{r_{kj}} \right] \quad (1)$$

where r_{kj} is the distance between matrix atom j (O, Si, or H) and site k of the adsorbate molecule. The first term in eq 1 is a Born−Mayer term corresponding to the short-range repulsive energy due to the finite compressibility of electron clouds when approaching the adsorbate at very short distances from the pore surface. Repulsive parameters A_{kj} and b_{kj} are obtained from mixing rules of like-atom pairs. (See below.) The second term in the above equation is a multipolar expansion series of the dispersion interaction that can be obtained from the quantum mechanical perturbation theory applied to intermolecular forces.[30] The multipolar expansion series was truncated after the first dispersion term C_6/r^6 in the present work. It has been shown that two-body dispersion coefficients C_{2n}^{kj} for isolated or condensed-phase species can be derived from the dipole polarizability α and the effective number of polarizable electrons N_{eff} of all interacting species, which are closely related to partial charges that can be obtained from ab initio calculations. f_{2n} represents damping functions that depend on the distance r_{kj} and the repulsive parameter b_{kj}:

$$f_{2n}(r_{kj}) = 1 - \sum_{m=0}^{2n} \left[\frac{b_{kj} r_{kj}}{m!} \right] \exp(-b_{kj} r_{kj}) \quad (2)$$

The role of these damping functions is to avoid the divergence of the dispersion interaction at short distances where the wave functions of the two species overlap (i.e., when the interacting species are in contact).[31] Each pair of interacting species is parametrized with the single b_{kj} repulsive parameter. The third term in eq 1 is the Coulombic interaction between the charge of site k and that of substrate atom j. The Coulomb energy was

(19) Coasne, B.; Pellenq, R. J. M. *J. Chem. Phys.* **2004**, *120*, 2013.
(20) Coasne, B.; Pellenq, R. J. M. *J. Chem. Phys.* **2004**, *121*, 3767.
(21) Coasne, B.; Gubbins, K. E.; Pellenq, R. J. M. *Part. Part. Syst. Charact.* **2004**, *21*, 149.
(22) MacElroy, J. M. D. *Langmuir* **1993**, *9*, 2682.
(23) Gelb, L. D.; Gubbins, K. E. *Langmuir* **1998**, *14*, 2097.
(24) Herdes, C.; Lin, Z.; Valente, A.; Coutinho, J. A. P.; Vega, L. F. *Langmuir* **2006**, *22*, 3097.
(25) Pellenq, R. J. M.; Levitz, P. E. *Mol. Phys.* **2002**, *100*, 2059.
(26) Puibasset, J.; Pellenq, R. J.-M. *J. Chem. Phys.* **2003**, *118*, 5613.
(27) Puibasset, J.; Pellenq, R. J.-M. *J. Phys.: Condens. Matter* **2004**, *16*, S5329.
(28) Coasne, B.; Alba-Simionesco, C.; Audonnet, F.; Dosseh, G.; Gubbins, K. E. *Adsorption* **2007**, *13*, 485.
(29) Coasne, B.; Alba-Simionesco, C.; Audonnet, F.; Dosseh, G.; Gubbins, K. E. *Langmuir* **2009**, *25*, 10648.
(30) Stone, A. *The Theory of Intermolecular Forces*; Clarendon: Oxford, U.K., 1996.
(31) Tang, K. T.; Toennies, J. P. *J. Chem. Phys.* **1984**, *80*, 3726.

Table 3. PN-TrAZ Potential Parameters for the Bean Model of the Nitrogen Molecule and Silica Species (a_0 = 0.529177 Å and E_h = 3.1578 × 10^5 K)

	nitrogen	silica		
atom	N	Si	O	H
q (e)	+0.482	+2	−1	+0.5
A (E_h)	139.1	6163.4	74.4	9.2
b (a_0^{-1})	1.931	2.395	2.190	2.122
α (a_0^3)	7.423	2.36	8.03	2.25
N_{eff}	3.187	1.529	4.656	0.324

Table 4. Dispersion and Repulsion Parameters for the Bean Model of the Nitrogen Molecule and Silica Species[a]

nitrogen species	silica species	C_6 ($E_h a_0^6$)	A (E_h)	b (a_0^{-1})
N	O	32.683	102.294	2.043
N	Si	9.861	925.995	2.138
N	H	6.174	86.948	2.392

[a] These parameters have been obtained in the framework of the PN-TrAZ model with Bohm and Ahlrichs combination rules for repulsive interactions.

computed using the Ewald summation technique. The atomic parameters and coefficients for the nitrogen/silica substrate interactions are given in Tables 3 and 4. The repulsive parameters for like pairs are taken from previous work by Pellenq and Nicholson for silicon[13] and from work by Filippini and Gavezzotti[32] for oxygen, hydrogen, and nitrogen. The repulsive cross-parameters were determined using the Bohm and Ahlrichs combination rules.[33] This type of potential function based on the PN-TrAZ parametrization method was used in various studies of molecular and covalent fluids at interfaces from open surfaces[26,34] to microporous zeolites[35−38] and more recently in the case of mesoporous silica materials.[26−29,39]

2.3. Grand Canonical Monte Carlo (GCMC). We performed GCMC simulations of nitrogen adsorption at 77 K on the atomistic silica nanopores shown in Figure 1. The GCMC technique is a stochastic method that simulates a system having a constant volume V (the pore with the adsorbed phase) in equilibrium with an infinite reservoir of particles imposing its chemical potential μ and temperature T.[40,41] The absolute adsorption isotherm is given by the ensemble average of the number of adsorbed atoms as a function of the pressure of the gas reservoir P. (The latter is obtained from the chemical potential μ according to the bulk equation of state for an ideal gas.) A Monte Carlo step in the present work corresponds to a particle displacement attempt and either a deletion or a creation attempt. Deletion and creation were attempted in the entire volume of the simulation box. The system was first allowed to equilibrate in the course of a GCMC run. Afterwards, the number of particles in the system and the isosteric heat of adsorption, which fluctuate about a steady value, were averaged using 10^5 Monte Carlo steps per particle. The uncertainty in the adsorbed amounts and the isosteric heat of adsorption is a few percent. (The latter corresponds to the statistical error in the set of data used to calculate the average values.) Because of their different intrinsic complexities, the pea and bean models have different computational efficiencies. Let us consider a simulation box in which a silica pore composed of N' atoms accommodates N nitrogen molecules. Once the total energy has been calculated, each Monte Carlo move involving one molecule (rotation, translation, deletion, or creation) requires a calculation of the energy with the $N-1$ other nitrogen molecules and the N' silica atoms. This leads to computational costs of $\sim N + N'$ for the pea model (one site) and $\sim 9N + 3N'$ for the bean model (three sites). As a result, depending on the number N' of silica atoms, the computational cost for the bean model is between 3 and 9 times larger than that for the pea model.

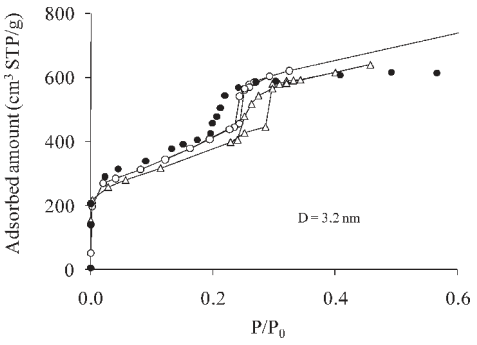

Figure 2. Nitrogen adsorption isotherm at 77 K in the silica cylindrical nanopore with D = 3.2 nm: (circles) pea model and (triangles) bean model. Pressures are reduced with respect to the saturating vapor pressure corresponding to the model chosen for the nitrogen molecule ($P_{0,pea}$ or $P_{0,bean}$). The black circles correspond to the experiments by Kruk et al.[43] for an MCM-41 nanopore with a diameter of D = 3.1 nm (with pressures reduced with respect to experimental saturating vapor pressure $P_{0,exp}$). Adsorbed amounts in the simulation data have been normalized to the experimental adsorbed amount when the pore is filled (∼600 cm³/STP per gram of adsorbent).

3. Results and Discussion

3.1. Adsorption Isotherm and Isosteric Heat of Adsorption. Adsorption isotherms for nitrogen at 77 K in nanoporous materials are usually plotted as a function of the reduced pressure P/P_0, where P_0 is the bulk saturating vapor pressure. Therefore, before presenting the simulation results for nitrogen adsorption at 77 K in regular cylindrical nanopores using the pea and bean models for the adsorbate molecule, an important discussion of the ability of the models to predict P_0 accurately is needed. On one hand, $P_{0,pea}$ = 1.23 bar for the pea model can be estimated using the Antoine law for Lennard-Jones fluids as determined by Kofke.[42] On the other hand, $P_{0,bean}$ = 0.87 bar for the bean model (TraPPE force field) was estimated by Herdes et al.[24] The latter values are, respectively, ∼20% larger and ∼10% lower than the experimental saturating vapor pressure, $P_{0,exp}$ = 1.01 bar. In what follows, we compare the simulated data with experimental data by using pressures reduced with respect to the saturating vapor pressure corresponding to the model chosen for the nitrogen molecule ($P_{0,pea}$ or $P_{0,bean}$).

The nitrogen adsorption isotherms obtained at 77 K for the regular cylindrical nanopores with D = 3.2 and 4.8 nm are shown in Figures 2 and 3, respectively. For each pore size, we report both

(32) Filippini, G.; Gavezzotti, A. *Acta Crystallogr.* **1993**, *B49*, 868.
(33) Bohm, H. J.; Ahlrichs, R. *J. Chem. Phys.* **1982**, *77*, 2028.
(34) Marinelli, F.; Grillet, Y.; Pellenq, R. J. M. *Mol. Phys.* **1999**, *97*, 1207.
(35) Lachet, V.; Boutin, A.; Tavitian, B.; Fuchs, A. H. *J. Phys. Chem. B* **1998**, *102*, 9224.
(36) Nicholson, D.; Pellenq, R. J. M. *Adv. Colloid Interface Sci.* **1998**, *76−77*, 179.
(37) Grey, T. J.; Nicholson, D.; Gale, J. D.; Peterson, B. K. *Appl. Surf. Sci.* **2002**, *196*, 105.
(38) Bichara, C.; Raty, J. Y.; Pellenq, R. J. M. *Phys. Rev. Lett.* **2002**, *89*, 016101.
(39) Pellenq, R. J. M.; Rousseau, B.; Levitz, P. E. *Phys. Chem. Chem. Phys.* **2001**, *3*, 1207.
(40) Allen, M. P.; Tildesley, D. J. *Computer Simulation of Liquids*; Clarendon: Oxford, U.K., 1987.
(41) Frenkel, D.; Smit, B. *Understanding Molecular Simulation: From Algorithms to Applications*, 2nd ed.; Academic Press: London, 2002.
(42) Kofke, D. *J. Chem. Phys.* **1993**, *98*, 4150.

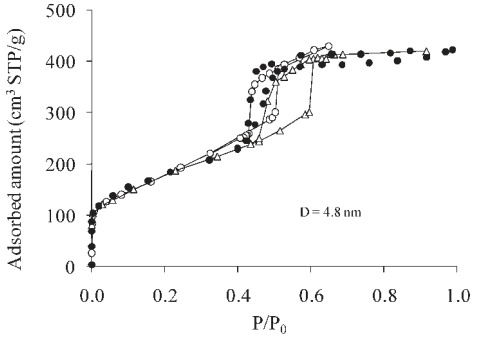

Figure 3. Nitrogen adsorption isotherm at 77 K in the silica cylindrical nanopore with $D = 4.8$ nm: (circles) pea model and (triangles) bean model. Pressures are reduced with respect to the saturating vapor pressure corresponding to the model chosen for the nitrogen molecule ($P_{0,pea}$ or $P_{0,bean}$). The black circles correspond to the experiments by Kruk et al.[43] for a MCM-41 nanopore with a diameter of $D = 4.6$ nm (with pressures reduced with respect to experimental saturating vapor pressure $P_{0,exp}$). Adsorbed amounts in the simulation data have been normalized to the experimental adsorbed amount when the pore is filled (~400 cm^3/STP per gram of adsorbent).

the data obtained with the pea and bean models of the nitrogen molecule. We also report in Figures 2 and 3 the experimental data obtained by Kruk et al.[43] for MCM-41 samples with similar pore diameters ($D = 3.1$ and 4.6 nm). Of course, the experimental data are reported in both cases with pressures in reduced units with respect to the experimental saturating vapor pressure, $P_{0,exp}$. Adsorbed amounts in the simulated adsorption isotherm have been normalized to the experimental adsorbed amount when the pore is filled (~600 cm^3/STP per gram of adsorbent for the sample with $D = 3.2$ nm and ~400 cm^3/STP per gram of adsorbent for the sample with $D = 4.8$ nm). Data obtained with the pea and bean models for the two pores conform to the typical behavior observed in the experiments for adsorption/condensation in MCM-41 cylindrical nanopores;[43] the adsorbed amount increases continuously in the multilayer adsorption regime until a jump occurs because of capillary condensation of the fluid within the pore. The condensation pressures for the nanopore with $D = 3.2$ nm are $P = 0.25P_{0,pea}$ for the pea model and $P = 0.29P_{0,bean}$ for the bean model whereas those for the nanopore with $D = 4.8$ nm are $P = 0.50P_{0,pea}$ for the pea model and $P = 0.58P_{0,bean}$ for the bean model. (A comparison with the experimental data will be discussed later.) Figure 4 shows for the pea model typical molecular configurations of nitrogen adsorbed at different pressures upon adsorption in the nanopores with $D = 3.2$ and 4.8 nm. We also show in Figure 5 typical molecular configurations obtained for these two nanopores with the bean model. Independently of the model used for the nitrogen molecule and the pore diameter, the surface of the silica nanopores is covered with a homogeneous film at the onset of capillary condensation. As expected for a regular nanopore, condensation occurs through an irreversible and discontinuous transition between the partially filled and completely filled configurations (which occurs when the adsorbed film becomes unstable).

The evaporation pressure for the nanopore with $D = 3.2$ is almost identical to the capillary condensation pressure for the pea model so that the pore filling is nearly reversible. In contrast, the evaporation pressure for this nanopore with the bean model, $P = 0.25P_{0,bean}$, is lower than the capillary condensation pressure

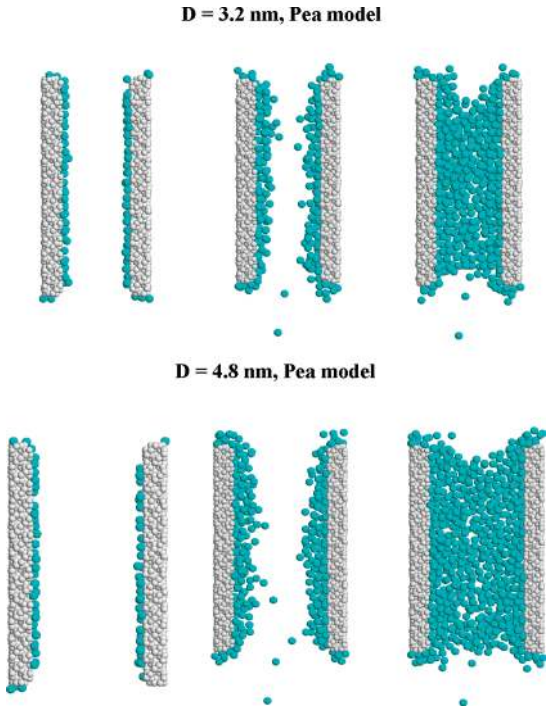

Figure 4. (Top) Typical molecular configurations for nitrogen in the silica cylindrical nanopore with $D = 3.2$ nm when the pea model is considered: (from left to right) $P = 2 \times 10^{-3}P_{0,pea}$, $0.24P_{0,pea}$, and $0.32P_{0,pea}$. The white spheres are the oxygen atoms of the silica nanopore, and the cyan spheres are the adsorbate molecule. (Bottom) Same as in the top image but for the nanopore with $D = 4.8$ nm: (from left to right) $P = 2 \times 10^{-3}P_{0,pea}$, $0.49P_{0,pea}$, and $0.61P_{0,pea}$.

so that a large hysteresis loop is observed. For the nanopore with $D = 4.8$ nm, the evaporation pressures are $P = 0.43P_{0,pea}$ for the pea model and $P = 0.47P_{0,bean}$ for the bean model. Whatever the model for the nitrogen molecule, the evaporation pressure for this nanopore is lower than the capillary condensation pressure so that large hysteresis loops are observed. In agreement with previous work on adsorption/desorption in cylindrical pores,[44−46] evaporation occurs through the displacement at equilibrium of a hemispherical meniscus along the pore axis (Figures 4 and 5). The hysteresis loops and the filling and emptying mechanisms observed in the present work are in agreement with the classical picture proposed long ago by Cohan;[47] the hysteresis loop is related to the different shapes of the gas/liquid interfaces encountered upon filling (cylindrical meniscus) and emptying (hemispherical meniscus) of the pores. By applying the classical Kelvin equation with these different meniscus shapes, one predicts that evaporation should occur at a pressure lower than condensation. In the framework of this theory, condensation is a metastable transition because the cylindrical gas/adsorbate interface upon adsorption is metastable with respect to the hemispherical gas/liquid interface (the hemispherical meniscus corresponds to the true equilibrium because it imposes phase coexistence of the confined gas and liquid phases).

The fact that for both the pea and bean models the hysteresis loop for the pore with $D = 4.8$ nm is much larger than that for the pore with $D = 3.2$ nm can be explained as follows. We know

(43) Kruk, M.; Jaroniec, M.; Kim, J. M.; Ryoo, R. *Langmuir* **1999**, *15*, 5279.

(44) Gelb, L. D. *Mol. Phys.* **2002**, *100*, 2049.
(45) Coasne, B.; Galarneau, A.; Di Renzo, F.; Pellenq, R. J.-M. *Langmuir* **2006**, *22*, 11097.
(46) Coasne, B.; Galarneau, A.; Di Renzo, F.; Pellenq, R. J.-M. *J. Phys. Chem. C* **2007**, *111*, 15759–15770.
(47) Cohan, L. H. *J. Am. Chem. Soc.* **1938**, *60*, 433–435.

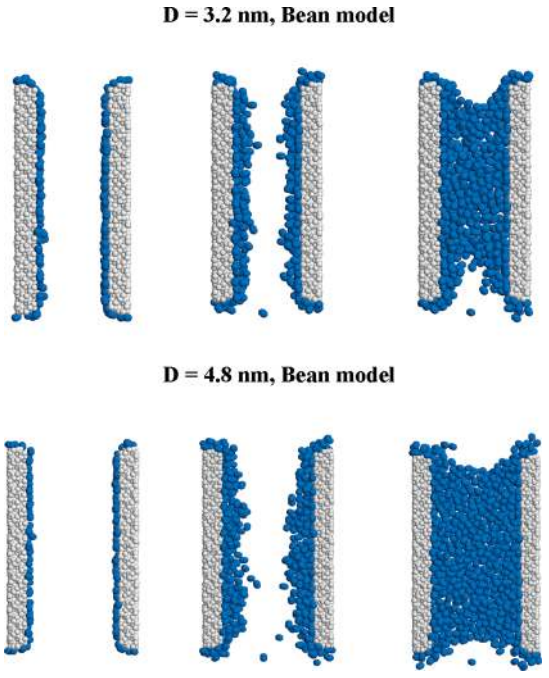

Figure 5. (Top) Typical molecular configurations for nitrogen in the silica cylindrical nanopore with $D = 3.2$ nm when the bean model is considered: (from left to right) $P = 0.003P_{0,bean}$, $0.25P_{0,bean}$, and $0.30P_{0,bean}$. The white spheres are the oxygen atoms of the silica nanopore, and the blue spheres are the nitogen atoms of the adsorbate molecule. (Bottom) Same as in the top image but for the nanopore with $D = 4.8$ nm: (from left to right) $P = 0.003P_{0,bean}$, $0.58P_{0,bean}$, and $0.61P_{0,bean}$.

from previous experimental,[48−51] theoretical,[52−55] and molecular simulation[44,56,57] work that there is a temperature, the so-called critical capillary temperature T_{cc}, above which capillary condensation in nanoporous solids becomes reversible. As the temperature approaches T_{cc}, the hysteresis loop shrinks and disappears for $T = T_{cc}$. We also know that T_{cc} increases as the pore diameter increases. Consequently, for a given temperature T, the hysteresis loop for the small nanopore ($D = 3.2$ nm) must be smaller than that for the large pore ($D = 4.8$ nm) because T is closer to T_{cc} for the small pore than that for the large pore. We note that this interpretation agrees with the experimental adsorption isotherms observed for MCM-41 samples; the adsorption isotherm is reversible for the nanopore with $D = 3.1$ nm whereas a hysteresis loop is observed for the nanopore with $D = 4.6$ nm. (See below for a more detailed comparison between experimental and simulated data.)

As mentioned above, data obtained with the pea and bean models conform to the typical experimental behavior for adsorption/condensation in cylindrical nanopores such as MCM-41 or SBA-15. The data obtained with the pea model better reproduce the experimental adsorption isotherms when pressures are plotted in reduced units with respect to the saturating vapor pressure of the model, $P_{0,pea}$. We note in passing that, when pressures are reduced with respect to $P_{0,exp}$, both the simulated adsorbed amounts prior to capillary condensation and simulated capillary condensation pressures for the bean model satisfactorily reproduce the experimental data (results not shown). Keeping in mind that neither the pea nor the bean model accurately reproduces the bulk saturating vapor pressure for nitrogen at 77 K, the results above show that the choice of the value for P_0 is crucial when one is interested in predicting the experimental data. As can be seen in Figures 2 and 3, there is a major discrepancy between the experimental data for the nanopore with $D = 3.1$ nm and the simulated data for the pea and bean models in the nanopore with $D = 3.2$ nm; the experimental adsorption isotherm is reversible, but the simulated adsorption isotherms are irreversible. This result can be partially attributed to the fact that for such pores ($D \approx 3.1-3.2$ nm) the temperature is close to the capillary critical temperature T_{cc} (i.e., a small change in the pore diameter causes the pore filling to change drastically from discontinuous and irreversible to continuous and reversible). This result is supported by the fact that the simulated hysteresis loop for the $D = 3.2$ nm nanopore with the pea model is very narrow, indicating that we are indeed close to the capillary critical temperature $T_{cc}(D)$ for this model. Other factors such as the uncertainty in the pore diameter (in the simulations as well as in the experiments), the pore shape (some authors have proposed in the literature that MCM-41 pores are slightly hexagonal as a result of the hexagonal ordering of the porosity), and the surface roughness might explain the differences between the simulated and experimental data. Adjusting the simulation parameters to fit the experimental data is beyond the scope of this article because it is a very tedious task (unless nonphysical fitting procedures are used to adjust the parameters). In particular, interaction potentials used in molecular simulations usually suffer from the absence of explicit many-body interactions and higher-order terms in the dispersion interaction. As a result, molecular simulation models provide a more global picture of gas adsorption and condensation in nanoporous materials than does a general quantitative characterization technique.

Figure 6 shows the isosteric heat Q_{st} for nitrogen adsorption at 77 K in the silica cylindrical nanopores with $D = 3.2$ and 4.8 nm. Q_{st} was obtained from fluctuations in the number of particles N in the system and from fluctuations in the internal energy U58

$$Q_{st} = RT - \frac{\partial\langle U\rangle}{\partial\langle N\rangle} = RT - \frac{\langle UN\rangle - \langle U\rangle\langle N\rangle}{\langle N^2\rangle - \langle N\rangle^2}$$

where T is the temperature and R is the rare gas constant. Data obtained with the pea and bean models are reported in Figure 6. Adsorbed amounts have been normalized to the total number of adsorbed molecules N_0 when the pore is filled. The use of adsorbed amounts as abscissae (instead of pressures) to plot the isosteric heat of adsorption curves helps us to avoid the choice of P_0. (See above.) For a given pore size, at low loading Q_{st} for the bean model is larger than that obtained for the pea model. This result shows that the bean model captures the attractive interaction between the nitrogen molecules and the hydroxyl groups of the silica surface. The isosteric heat of adsorption curve for the pea model is characteristic of the adsorption of simple gases on homogeneous surfaces; $Q_{st} \approx 11$ kJ/mol is almost constant upon the adsorption of the first monolayer and then decreases to a value close to the heat of liquefaction of nitrogen (5.6 kJ/mol) as further

(48) Burgess, C. G. V.; Everett, D. H.; Nuttall, S. *Langmuir* **1990**, *6*, 1734.
(49) Morishige, K.; Fujii, H.; Uga, M.; Kinukawa, D. *Langmuir* **1997**, *13*, 3494.
(50) Morishige, K.; Ito, M. *J. Chem. Phys.* **2002**, *117*, 8036.
(51) Trens, P.; Tanchoux, N.; Galarneau, A.; Brunel, D.; Fubini, B.; Garrone, E.; Fajula, F.; Di Renzo, F. *Langmuir* **2005**, *21*, 8560.
(52) Nakanishi, H.; Fisher, M. *J. Chem. Phys.* **1983**, *78*, 3279.
(53) Evans, R.; Marini Bertollo Marconi, U.; Tarazona, P. *J. Chem. Phys.* **1986**, *84*, 2376.
(54) Ball, P. C.; Evans, R. *Langmuir* **1989**, *5*, 714.
(55) Woo, H. J.; Monson, P. A. *Phys. Rev. E* **2003**, *67*, 041207.
(56) Coasne, B.; Gubbins, K. E.; Pellenq, R. J. M. *Adsorption* **2005**, *11*, 289.
(57) Pellenq, R. J. M.; Coasne, B.; Denoyel, R.; Puibasset, J. *Stud. Surf. Sci. Catal.* **2007**, *160*, 1–8.
(58) Nicholson, D.; Parsonage, N. G. *Computer Simulation and the Statistical Mechanics of Adsorption*; Academic Press: London, 1982.

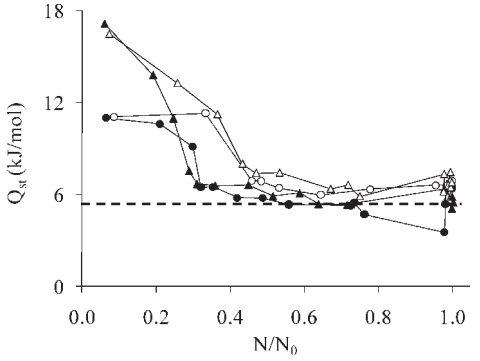

Figure 6. Isosteric heat Q_{st} for nitrogen adsorption at 77 K in silica cylindrical nanopores. (Circles) Pea model and (triangles) bean model. Open and closed symbols correspond to pores with D = 3.2 and 4.8 nm, respectively. Adsorbed amounts have been normalized to the total number N_0 of adsorbed molecules when the pore is filled. The dashed line indicates the heat of liquefaction for nitrogen at 77 K.

adsorption takes place. In contrast, the isosteric heat of adsorption curve for the bean model is characteristic of adsorption on heterogeneous surfaces; Q_{st} decreases continuously upon increases in the adsorbed amount. Interestingly, as in the case of the pea model, Q_{st} for the bean model decreases from ~14 kJ/mol at low loading down to a value close to the heat of liquefaction of nitrogen (6−7 kJ/mol). The fact that both the pea and bean models lead to similar Q_{st} values at high loadings suggests that the main difference between these two models lies in the description of the effect of surface heterogeneity on the adsorption of the first monolayers. In particular, we note that both models are in good agreement with the experimental isosteric heat of condensation (~6 kJ/mol) estimated by Trens et al. for nitrogen at 77 K in MCM-41 nanopores.[59] On one hand, the nitrogen molecule in the pea model "sees" a homogeneous silica surface because of the consideration of only the oxygen atoms in this model. In contrast, the nitrogen molecule in the bean model is sensitive to the surface heterogeneity of the silica pores because they interact with all of the atoms of the substrate in this model. The results above show that, although the data for the pea model reasonably describe the experimental data, the bean model provides a more realistic picture of nitrogen adsorption in the vicinity of silica surfaces or confined in silica nanopores. No experimental isosteric heat of adsorption curve is available in the literature for nitrogen at 77 K in MCM-41 nanopores. This is due to the fact that the latter measurements require adsorption experiments to be performed at temperatures above and below 77 K. Temperatures above this temperature can be easily reached by heating the thermal bath in which the experimental cell is introduced. (The thermal bath usually consists of liquid argon at 87 K or liquid nitrogen at 77 K.) In contrast, reaching temperatures below 77 K is not simple because it requires cooling of the thermal bath. Although no experimental isosteric heat data are available, comparison with isosteric heat of adsorption curves for other gases in MCM-41 clearly shows that the behavior observed for the bean model better captures the qualitative experimental behavior. (See the experimental data for argon in Figure 3 of ref 60 and for tert-butyl alcohol in Figure 6 of ref 51.) In particular, the experimental isosteric heat of adsorption curve is characteristic of adsorption on heterogeneous surfaces as Q_{st} decreases continuously with increasing adsorbed amount, in qualitative agreement with the simulated data for the bean model.

In this work we also compared the structure of confined nitrogen for both the pea and bean models. Figure S1 in the Supporting Information shows density profiles $\rho(r)$ for nitrogen confined at 77 K in the silica cylindrical nanopore with D = 3.2 nm at the onset of capillary condensation and after capillary condensation when the pore is filled. Data for the pea and bean models are reported. Similar results have been obtained for the nanopore with D = 4.8 nm, so they are not reported for the sake of brevity and clarity. We recall that the size of the nitrogen molecule in the pea model is σ = 0.375 nm whereas that in the bean model corresponds to two Lennard-Jones spheres with σ = 0.331 nm separated by a distance of 0.11 nm. The density profiles obtained at the onset of capillary condensation show that a molecular layer of nitrogen is already adsorbed at the silica surface and that a second layer started to form. Above capillary condensation, the confined liquid phase also exhibits density oscillations (up to five layers are confined when the pore is filled). Such a spatial ordering of fluids in the vicinity of surfaces or confined in porous materials have been discussed in detail in the literature. (For a review, see ref 61.) Both at the onset and above capillary condensation, the density profiles obtained for the pea and bean models are similar (strong layering of the confined adsorbate and the same number of confined layers with similar density amplitudes). Figure S2 in the Supporting Information shows the pair correlation functions $g(r)$ for nitrogen confined above capillary condensation in the silica cylindrical nanopore with D = 3.2 nm. Data for the pea and bean models are reported. We also report the pair correlation function obtained for each model for bulk nitrogen at 77 K. Again, similar results have been obtained for the nanopore with D = 4.8 nm, so they are not reported for the sake of brevity and clarity. All of the pair correlation functions for the confined fluid have been corrected for the excluded volume effect according to the method reported by Gallo et al.[62,63] The $g(r)$ function between molecules A and B is related to the probability of having a molecule A at a distance between r and $r + dr$ from an atom B. Note that this function is also related to the inverse Fourier transform of the structure factor $S(q)$ measured in X-ray or neutron diffraction. The pair correlation functions for the pea and bean models show that the confined fluid has a liquidlike structure, where only short-range positional order is observed. It is found that the peaks of the $g(r)$ function for the confined molecules are located at the same positions as those for the bulk fluid. The $g(r)$ function for the pea model is almost identical to that for the bean model, which shows that such a simple model is able to capture the structure and organization of the confined fluid.

3.2. Surface Area and Pore Size Distribution Determination. We now discuss the use of the BET method to assess the specific surface area of a nanoporous material from adsorption data. The BET method is one of the most widely used methods in the field of porous solid characterization. It allows one to estimate specific surfaces from adsorption isotherms on the basis of a model developed to describe multilayer adsorption. The hypotheses of the model are that (1) adsorption occurs on energetically homogeneous sites having an energy ε_1 (the surface density of sites is also constant) and (2) molecules can adsorb on each other. In the latter case, the adsorption energy ε_0 for all molecules adsorbed above the first layer is constant and equal to the cohesion energy

(59) Trens, P.; Tanchoux, N.; Galarneau, A.; Brunel, D.; Fubini, B.; Garrone, E.; Fajula, F.; Di Renzo, F. *Langmuir* **2005**, *21*, 8560.
(60) Neimark, A. V.; Ravikovitch, P. I.; Grun, M.; Schuth, F.; Unger, K. K. *J. Colloid Interface Sci.* **1998**, *207*, 159.
(61) Evans, R. *J. Phys.: Condens. Matter* **1990**, *2*, 8989.
(62) Gallo, P.; Ricci, M. A.; Rovere, M. *J. Chem. Phys.* **2002**, *116*, 342.
(63) Alba-Simionesco, C.; Dosseh, G.; Dumont, E.; Frick, B.; Geil, B.; Morineau, D.; Teboul, V.; Xia, Y. *Eur. Phys. J. E* **2003**, *12*, 19.

Table 5. BET Surface (S_{BET}) and Energy Parameter C Obtained from Nitrogen Adsorption at 77 K in Cylindrical Silica Nanopores with Diameters of D = 3.2 and 4.8 nm[a]

	D = 3.2 nm (S_{GEO} = 134 nm^2)		D = 4.8 nm (S_{GEO} = 197 nm^2)	
model	pea	bean	pea	bean
S_{BET} (nm^2)	106	120	165	174
C	59	89	67	116

[a] The data obtained with the pea and bean models are reported. We used $a(N_2)$ = 0.135 nm^2 for the molecular surface area for a nitrogen molecule at 77 K. For each pore, the true geometrical surface S_{GEO} is indicated. The linear ranges of data between $0.04P_0$ and $0.2P_0$ for the nanopore with D = 3.2 nm and between $0.04P_0$ and $0.4P_0$ for the nanopore with D = 4.8 nm were considered to estimate the BET surface as well as the C parameter. (See Figure S3 in the Supporting Information.)

in the bulk liquid. With these assumptions, it can be shown that the adsorption data (adsorbed amount N versus relative pressure P/P_0) must obey the following equation

$$\frac{\frac{P}{P_0}}{N\left(1-\frac{P}{P_0}\right)} = \frac{1}{N_0 C} + \frac{C-1}{N_0 C}\frac{P}{P_0} \quad (3)$$

where N_0 is the monolayer capacity (i.e., the number of atoms needed to cover the substrate uniformly with one complete monolayer). The factor C is related to the adsorption energies in the system, $C = [(\varepsilon_1 - \varepsilon_0)/k_B T]$ where k_B is the Boltzmann constant and T is the temperature. Parameters C and N_0 can be estimated from the slope and the intercept of the BET plot given by eq 3.

Figure S3 in the Supporting Information shows the BET plots corresponding to the nitrogen adsorption isotherms (77 K) for the pea and bean models in the silica nanopores with D = 3.2 and 4.8 nm. A comparison between the BET surface, S_{BET}, and the geometrical surface, S_{GEO}, is reported in Table 5 for each model and nanopore. The geometrical surface has been estimated as the pore circumference multiplied by the pore length. For each nanopore, we also report in Table 5 the value of C. The monolayer capacity has been converted into a surface area using the molecular surface area for a nitrogen molecule at 77 K, $a(N_2)$ = 0.135 nm^2. Galarneau et al.[64] have shown that the latter value should be preferred to the common value of 0.162 nm^2 when considering templated mesoporous silicas. In agreement with the experiments for MCM-41,[43] we found that the BET plots corresponding to our data for nitrogen adsorption in the silica nanopores follow the expected linear behavior in the relative pressure range of 0.04−0.2 for the nanopore with D = 3.2 nm and 0.04−0.4 for the nanopore with D = 4.8 nm. For both the nanopores with D = 3.2 and 4.8 nm, BET surface S_{BET} obtained with the bean model is in good agreement with true geometrical surface S_{GEO} (within ∼10%). Moreover, the values obtained for C with the bean model are consistent with the experimental values that are usually reported in the literature for oxide surfaces, ∼80−150.[8] However, the BET surfaces obtained for the pea model underestimate the true geometrical surfaces of the silica nanopores by about 15−20%. The values obtained for C with the pea model are also lower that those observed in experiments on MCM-41 samples (80−110).[64] We note that good agreement is reached between the BET surfaces obtained for the pea model and the true geometrical surfaces if the common value of $a(N_2)$ = 0.162 nm^2 is used for the molecular surface area for a nitrogen molecule at 77 K. Given that experiments have shown that $a(N_2)$ = 0.135 nm^2 should be used to estimate the surface area of templated mesoporous silicas accurately, the fact that the BET surfaces estimated for the bean model with this value are close to the true surface of the nanopores suggests that this model provides a realistic description of nitrogen adsorption in these materials.

We now discuss on the basis of our simulated data the ability of pore size evaluation methods to relate the pore radius to the capillary condensation and evaporation pressures. Table 6 shows the relative condensation and evaporation pressures, P_C and P_E, obtained for the pea and bean models of nitrogen at 77 K in silica nanopores with D = 3.2 and 4.8 nm. Capillary condensation and evaporation pressures in nanopores are usually described using the modified Kelvin equation.[8] To account for the effect of curvature, we corrected the values of the surface tension in the Kelvin equation using the Tolman equation

$$\gamma(R) = \gamma(\infty)\left(1+\frac{\alpha\delta}{R}\right) \quad (4)$$

where $R = R_0 - t(P)$, which corresponds to the pore radius diminished by the thickness of the adsorbed film, is the radius of curvature of the gas/liquid interface at the condensation or evaporation pressure. α is the shape factor that equals 1 upon adsorption (cylindrical adsorbed film) and 2 upon desorption (hemispherical meniscus along the pore axis). We used $\delta = 0.2\sigma$ (where σ = 3.75 Å is the kinetic diameter of the nitrogen molecule); such a Tolman length is consistent with the typical values reported in the literature that correspond to a small fraction of the size of the molecule.[65−68] Even for a large nanopore of a diameter D = 4.8 nm where the modified Kelvin equation is expected to become accurate, the latter equation overestimates by at least ∼15% the condensation and evaporation pressures. We note that the condensation and evaporation pressures found in the GCMC simulations can be fitted using the modified Kelvin equation only when a large Tolman length of $\delta \approx \sigma$ is used. This result is consistent with our previous work[69] for argon adsorption in silica nanopores in which we reported that a large unphysical Tolman length ($2\delta \approx 6\sigma$) must be used in the modified Kelvin equation to account for the capillary condensation and evaporation pressures found in the simulations. The results above show that the charaterization methods based on the analysis of the adsorption and desorption branch using the modified Kelvin equation overestimate the condensation and evaporation pressures (reciprocally, the modified Kelvin equation underestimates the pore size of the material for a given transition pressure). These results are consistent with previous work in which it was reported that the Kelvin equation breaks down for pores having a diameter smaller than $D \approx 15\sigma$ (again, σ is the size of the adsorbate).[70−73]

(64) Galarneau, A.; Cambon, H.; Di Renzo, F.; Fajula, F. *Langmuir* **2001**, *17*, 8328.
(65) Bykov, T. V.; Zeng, X. C. *J. Phys. Chem. B* **2001**, *105*, 11586.
(66) Lei, Y. A.; Bykov, T. V.; Yoo, S.; Zeng, X. C. *J. Am. Chem. Soc.* **2005**, *127*, 15346.
(67) Anisimov, M. A. *Phys. Rev. Lett.* **2007**, *98*, 035702.
(68) van Giessen, A. E.; Blokhuis, E. M.; Bukman, D. J. *J. Chem. Phys.* **1998**, *108*, 1148.
(69) Coasne, B; Galarneau, A.; Di Renzo, F.; Pellenq, R. J. M. *Adsorption* **2008**, *14*, 215.
(70) Fisher, L. R.; Israelachvili, J. N. *J. Colloid Interface Sci.* **1981**, *80*, 528.
(71) Celestini, F.; Pellenq, R.J.-M.; Bordarier, P.; Rousseau, B. *Z. Phys. D* **1996**, *37*, 49.
(72) Celestini, F. *Phys. Lett. A* **1997**, *228*, 84.
(73) Walton, J. P. R. B; Quirke, N. *Mol. Simul.* **1989**, *2*, 361.
(74) Pellenq, R. J. M.; Coasne, B.; Denoyel, R. O.; Coussy, O. *Langmuir* **2009**, *25*, 1393.

Table 6. Simulated Condensation and Evaporation Relative Pressures (P_C, P_E) and Film Thickness in angstroms at the Transition (t(P_C), t(P_E)) for Nitrogen Adsorbed at 77 K in Silica Nanopores with Diameters of D = 3.2 and 4.8 nm[b]

	D = 3.2 nm				D = 4.8 nm			
	P_C	t(P_C)	P_E	t(P_E)	P_C	t(P_C)	P_E	t(P_E)
	simulation data							
pea model	0.25	6.4	0.25	6.4	0.50	10.6	0.43	8.8
bean model	0.29	7.2	0.25	6.3	0.58	11.3	0.47	8.4
PCDC[a]					0.52	11.0	0.38	7.3

[a] See ref 74 for details. [b] The data for the pea and bean models are shown. We also show a comparison with the values expected on the basis of the modified Kelvin equation and the model PCDC. (See the text.) Note that the surface tension in the Kelvin equation has been corrected according to the Tolman equation to account for the curvature effect. (See eq 4.)

Recently, some of us reported a simple phenomenological model that describes the adsorption and capillary condensation and evaporation of pure fluids confined in regular cylindrical nanopores.[74] In this model, which we call the PCDC model in what follows, the free-energy density of the system is derived using interfacial tensions and a corrective term that accounts for the interaction coupling between the vapor/adsorbed liquid and the adsorbed liquid/adsorbent interfaces. This model, which is based on the original work by Celestini,[72] proposes that capillary condensation and evaporation are metastable and equilibrium processes, respectively, hence exhibiting the existence of a hysteresis loop in adsorption/desorption isotherms. We also extended this phenomenological model to give a quantitative description of adsorption on the pore wall and hysteresis width evolution with temperature and confinement. Used as a characterizing tool, this integrated model allows a single fit of an experimental adsorption/desorption isotherm assessing essential characterization data such as the specific surface area, pore volume, and pore size distribution. In particular, in contrast to the modified Kelvin equation, the PCDC model does not require the inclusion of additional data such as the pressure dependence of the adsorbed film thickness, t(P). Table 6 compares the simulated condensation and evaporation pressures (P_C, P_E) for nitrogen at 77 K in the silica nanopores with diameters D = 3.2 and 4.8 nm with the predictions of the PCDC model. We also report the predictions of the PCDC model for the thickness of the film adsorbed at the onset of capillary condensation and upon desorption at the evaporation pressure. Only predictions for the nanopore with a diameter of D = 4.8 nm are shown because the PCDC model does not apply to critical adsorption isotherms such as that for the nanopore with D = 3.2 nm (i.e., showing continuous and reversible filling of the nanopore). Indeed, the experimental adsorption isotherm for this pore size is reversible, which indicates that the temperature is below that the capillary critical temperature T_{cc}. For such critical adsorption isotherms, molecular simulations have shown that although there is preferential adsorption near the pore surface, no clear interface between the adsorbed film and the gas phase in the pore center is observed. As a result, the PCDC model should not be used to describe critical adsorption isotherms because it explicitly assumes vapor/adsorbed liquid and adsorbed liquid/adsorbent interfaces. This last statement also applies to the Kelvin equation or other models proposed in the literature[74−78] in which phase coexistence among the adsorbed, gas, and solid phases is assumed. Coming back to the comparison with the simulations, the PCDC model is in fair agreement with the data for the pea and bean models for the adsorbed film thickness (within ~1 Å). The condensation pressure is also reasonably predicted by the PCDC model (to ~10%). The evaporation pressure in the PCDC model, which underestimates that for the bean model, is in good agreement with the experimental data and the simulated data for the pea model. Knowing that the small number of adjustable parameters in the PCDC model has been refined to fit the experimental data, the fact that the model accurately describes the simulated data for the pea model is consistent with the agreement found between this set of simulations and the experiments (Figure 3).

4. Conclusions

Data obtained with the pea and bean models conform to the typical experimental behavior for the adsorption/condensation of nitrogen in MCM-41 cylindrical nanopores; the adsorbed amount increases continuously in the multilayer adsorption regime until an irreversible jump occurs as a result of capillary condensation and evaporation of the fluid within the pore. The surface of the silica nanopores is covered by a molecularly thick film at the onset of capillary condensation, and condensation occurs through an irreversible discontinuous transition between the partially filled and the completely filled configurations. In contrast, evaporation occurs at equilibrium through the displacement of a hemispherical meniscus along the pore axis. Comparison with the experimental data is not trivial because neither the pea nor the bean model accurately reproduces the bulk experimental saturating vapor pressure, $P_{0,exp}$ = 1.01 bar. P_0 for the pea model is ~20% larger than $P_{0,exp}$ whereas P_0 for the bean model is ~10% lower than $P_{0,exp}$. When the simulated data are plotted with pressure in reduced units with respect to the saturating vapor pressure corresponding to the model, $P_{0,pea}$ and $P_{0,bean}$, the data obtained with the pea model better reproduce the experimental adsorption isotherms. A major difference between the pea and bean models for nitrogen adsorption at low temperature concerns the isosteric heat of adsorption curves Q_{st}. Q_{st} as a function of loading for the pea model is characteristic of adsorption on homogeneous surfaces because it is almost constant upon adsorption of the first monolayer and then sharply decreases as further adsorption takes place. In contrast, Q_{st} for the bean model is characteristic of adsorption on heterogeneous surfaces as Q_{st} decreases continuously with increasing adsorbed amount. The results above show that, although the data for the pea model reasonably describe the experimental data, the bean model provides a more realistic picture of nitrogen adsorption in the vicinity of silica surfaces or confined in silica nanopores. In particular, the bean model is sensitive to the surface corrugation and surface chemistry (silanol groups and siloxane bridges) of the silica nanopores. The results above suggest that the pea model can be used for characterization purposes when one is interested in capturing the experimental behavior upon adsorption and desorption in silica nanopores with various morphologies (pore geometry) and topologies (independent or connected pores). However, the bean model is more suitable to investigating in a qualitative way the details of the interaction with the surface because this model, which accounts for the partial charges located on the nitrogen atoms of the molecule (quadrupole), allows for a description of the specific interactions involved in this adsorbate and silica surfaces (silanol groups and siloxane bridges) or grafted silica surfaces.

(75) Cole, M. W.; Saam, W. F. *Phys. Rev. Lett.* **1974**, *32*, 985.
(76) Zarragoicoechea, G. J.; Kuz, A. V. *Phys. Rev. B* **2002**, *65*, 021110.
(77) Chen, Y.; Aranovich, G. L.; Donohue, M. D. *J. Colloid Interface Sci.* **2007**, *307*, 34.
(78) Miyahara, M.; Kanda, H.; Yoshioka, T.; Okazaki, M. *Langmuir* **2000**, *16*, 4293.

In conclusion, we discuss in the general context of the characterization of porous solids the ability of the different models considered in this work to describe nitrogen adsorption in silica materials. Each of these models has its main advantages and disadvantages. For instance, the PCDC model is a general comprehensive thermodynamic approach that describes adsorption and capillary condensation in nanopores as well as the disappearance of the capillary hysteresis loop as the temperature reaches the capillary critical temperature. However, although this model provides a reasonable semiquantitative description of nitrogen adsorption experiments in regular nanoporous silicas (within an error of ca. 10−20%), it does not include surface roughness and morphological disorder effects that are encountered for any experimental sample. In contrast to simple thermodynamic models, molecular simulations (with either the pea or bean model) can be used for characterization purposes where one is interested in capturing the behavior for nitrogen in any ordered or disordered silica nanoporous material. As mentioned above, the pea model allows a description of the global adsorption isotherm for nitrogen whereas the more sophisticated bean model is more suitable to investigating the details of the interaction with the surface. As a general conclusion, we emphasize that, whatever the model considered to describe nitrogen adsorption in nanoporous silicas (thermodynamic approaches, density functional theory, molecular simulations, etc.), it is not possible to reproduce experimental data very accurately (say within a percent) unless nonphysical fitting procedures are used to adjust the parameters. Indeed, besides the uncertainties in the experimental samples (morphology, topology, surface roughness, chemical heterogeneity, pore size, and shape distributions), the models mentioned above suffer from limitations that arise from the use of mean-field approximations (in the case of density functional theory), the absence of explicit many-body interactions, a simple description of the nanoporous materials, and so forth. As a result, the latter models provide a global picture of gas adsorption and condensation in nanoporous materials rather than a general quantitative characterization technique.

Acknowledgment. The molecular simulations were performed on local workstations that were purchased with funding from ANR research project SIMONANOMEM (ANR-07-NANO-055) and the CNRS-ATILH Contrat de Programme de Recherche: Résistance, Porosité et Transport des Matériaux Cimentaires.

Supporting Information Available: Additional simulation results. This material is available free of charge via the Internet at http://pubs.acs.org.